

## Finite-temperature density matrix renormalization using an enlarged Hilbert space

Adrian E. Feiguin and Steven R. White

*Department of Physics and Astronomy, University of California, Irvine, California 92697, USA*

(Received 5 October 2005; published 2 December 2005)

We apply a generalization of the time-dependent density matrix renormalization group (DMRG) to study finite-temperature properties of several quantum spin chains, including the frustrated  $J_1$ - $J_2$  model. We discuss several practical issues with the method, including use of quantum numbers and finite-size effects. We compare with transfer-matrix DMRG, finding that both methods produce excellent results.

DOI: [10.1103/PhysRevB.72.220401](https://doi.org/10.1103/PhysRevB.72.220401)

PACS number(s): 71.27.+a, 71.10.Pm, 72.15.Qm, 73.63.Kv

The density matrix renormalization group (DMRG) method<sup>1</sup> provides extremely accurate information about the ground state of one-dimensional (1D) systems. To study thermodynamic properties, it was subsequently adapted to calculate the transfer matrix of a 1D quantum system. In the transfer-matrix DMRG (TM-DMRG) method,<sup>2,3</sup> the usual DMRG sweeping takes place in the imaginary time direction, whereas the thermodynamic limit in one spatial direction is automatically obtained by targeting the maximum transfer matrix eigenvalue and eigenvector. TM-DMRG gives excellent results, but is also technically somewhat more difficult than ordinary DMRG, in part because the transfer matrix is non-Hermitian. A robust finite-temperature method based on the original DMRG method would be very useful, if only because DMRG and TM-DMRG have slightly different strengths and weaknesses.

In the past year, ideas from the quantum information field have greatly extended the capabilities of DMRG.<sup>4-7</sup> The first major advance was a different approach to real-time evolution within a generalized DMRG framework (consisting of matrix-product states<sup>8</sup>), and shortly thereafter within a standard DMRG framework.<sup>9,10</sup> Subsequently, Zwolak and Vidal, and Verstraete *et al.*, separately, devised methods allowing finite-temperature DMRG. The approach of Zwolak and Vidal introduced the idea of a matrix-product description of density operators, rather than of wave functions. Within the density operator formulation, the infinite temperature system is trivial to describe, and imaginary time evolution is used to reach finite temperature. Verstraete *et al.*<sup>11</sup> argued that a more efficient procedure is to enlarge the Hilbert space with auxiliary sites (called ancillas), and to evolve in imaginary time a pure state within the larger space. The auxiliary states act as a perfect heat bath, and when traced out give exact thermodynamic averages.

The ancilla approach is especially convenient from the traditional DMRG point of view. A wave-function description is usually more familiar and comfortable than a density operator description. The ancillas appear geometrically as another chain parallel to the first, making the system resemble a ladder. More generally, the ancillas form a copy of the original system, doubling the size of the lattice. As we discuss below, the ancilla states can be given quantum numbers, increasing the efficiency of the calculation. In this paper, we apply the ancilla approach to study the thermodynamics of several spin chains. We consider practical issues such as finite-size effects, and compare our results with TM-DMRG.

The use of auxiliary systems to study thermodynamics in quantum systems originated as a key idea in thermo field dynamics.<sup>12-14</sup> Let the energy eigenstates of the system in question be  $\{n\}$ . Introduce an auxiliary set of fictitious states  $\{\tilde{n}\}$  in one-to-one correspondence with  $\{n\}$ . Define the unnormalized pure quantum state, in an enlarged Hilbert space,

$$|\psi(\beta)\rangle = e^{-\beta H/2} |\psi(0)\rangle = \sum_n e^{-\beta E_n/2} |n\tilde{n}\rangle, \quad (1)$$

where  $\tilde{n}$  is the matching state to  $n$ ,  $\beta$  is the inverse temperature, and  $|\psi(0)\rangle = \sum_n |n\tilde{n}\rangle$  is our thermal vacuum. Note that the Hamiltonian only applies to the real sites; the ancillas evolve only through their entanglement acting as a thermal bath. Then the partition function is

$$Z(\beta) = \langle \psi | \psi \rangle \quad (2)$$

and we can obtain the exact thermodynamic average of an operator  $A$  (acting only on the real states), as

$$\langle A \rangle = Z(\beta)^{-1} \langle \psi | A | \psi \rangle. \quad (3)$$

At  $\beta=0$ , the state  $\psi$  is the maximally entangled state between the real system and the fictitious system. If we change basis from the energy eigenstates  $n$  to some other arbitrary basis  $s$ ,  $\psi$  is still maximally entangled,<sup>13</sup>  $|\psi(0)\rangle = \sum_s |s\tilde{s}\rangle$ . A natural basis to use is the site basis, where the state of each site  $i$  takes on a definite value  $s_i$ . One finds

$$|\psi(0)\rangle = \prod_i \sum_{s_i} |s_i \tilde{s}_i\rangle = \prod_i |I_{0i}\rangle \quad (4)$$

defining the maximally entangled state  $|I_{0i}\rangle$  of site  $i$  with its ancilla.

From the DMRG point of view, the maximally entangled state between the left and right blocks would be the worst possible state to try to represent; all density matrix eigenvalues would be equal. If one split the system between the real sites on one side and the ancilla on the other, one would have exactly this worst case at  $\beta=0$ . It is remarkable that, if one pairs each site with its ancilla, and splits the system in two respecting this pairing, the infinite temperature state is the best possible state for DMRG, with only one density matrix eigenvalue being nonzero. This leads to the natural ordering of sites for DMRG site 1, ancilla 1, site 2, ancilla 2, etc. Alternatively, one can group together a site and its ancilla into a supersite. Although the dimension of the superblock is

larger with supersites, next-nearest neighbor interactions are not generated by the ancilla, simplifying the time evolution. In our simulations we have used supersites.

In order to utilize conserved quantum numbers, it is useful to think of each ancilla as being the antisite of its site. A state of the ancilla is given opposite quantum numbers to the corresponding state of the real site. In this way, the state of interest has both total charge and total  $z$  component of spin equal to zero. In the case of the spin-1/2 chain, for instance, the antisite is just another spin-1/2 site. We choose a local representation for the supersite “spin+ancilla” with the states  $|I_0\rangle = (|\uparrow, \downarrow\rangle + |\downarrow, \uparrow\rangle)/\sqrt{2}$ ,  $|I_1\rangle = (|\uparrow, \downarrow\rangle - |\downarrow, \uparrow\rangle)/\sqrt{2}$ ,  $|I_2\rangle = |\uparrow, \uparrow\rangle$ , and  $|I_3\rangle = |\downarrow, \downarrow\rangle$ , where the first arrow in each term designates the real site. The initial state  $|\psi(0)\rangle$  is then constructed by using Eq. (4) with the triplet  $|I_0\rangle$  on every position along the chain. As a result, we obtain an equivalent one-dimensional chain with four states per site. The other states  $|I_1\rangle$ ,  $|I_2\rangle$ , and  $|I_3\rangle$  appear during the time evolution from the exchange terms in  $H$ . This idea can be generalized to arbitrary spin, or to fermions by means of a particle-hole transformation.

The essence of the ancilla finite-temperature method is to start in this local  $\beta=0$  state, and evolve in imaginary time through a succession of temperatures  $\beta$ . To evolve in time, we utilize one of the recently developed time evolution methods, which perform equally well in imaginary time. The most efficient of these utilizes a Suzuki-Trotter breakup of the Hamiltonian, and each DMRG step consists of evolving the state using the link evolution operator  $\exp(-\tau H_{i,i+1}/2)$  between the two central sites.<sup>9,10</sup> This method requires nearest neighbor interactions, at least in its simplest form. Alternatively, one can evolve in a basis optimized for a single time step by solving explicitly the corresponding differential equation,<sup>15</sup> which does not require local interactions but is less efficient. Notice again that  $H$  does not act on the ancillas and that the ancillas in the system block are not traced out in the construction of the density matrix. When the environment block is traced out, its ancilla states, which are mixed in with its real states, are automatically traced out. The measurement of thermodynamic averages using Eq. (3) automatically traces out all ancillas, since the measurement operators do not refer to them.

The infinite temperature starting state has a correlation length of 0 and requires only one state per block. As the system evolves in imaginary time, longer range entanglement is produced and the correlation length grows. The number of states needed for a given accuracy grows as the temperature decreases. It is most natural to slowly increase the size of the basis, in order to keep a roughly constant truncation error. One may wish to set a minimum basis set size to make the early evolution essentially exact with little computational cost. In the test calculations below we kept the truncation error below  $10^{-10}$ , which in the systems considered corresponded typically to a maximum of  $m=500$  DMRG states. It turns out that most of these states have  $S^z=0$ , and therefore the total size of the basis is of the order of  $10^6$  states for the spin- $\frac{1}{2}$  Heisenberg chain. In more difficult systems one would use a less stringent error criterion. In order to determine convergence, we have compared the specific

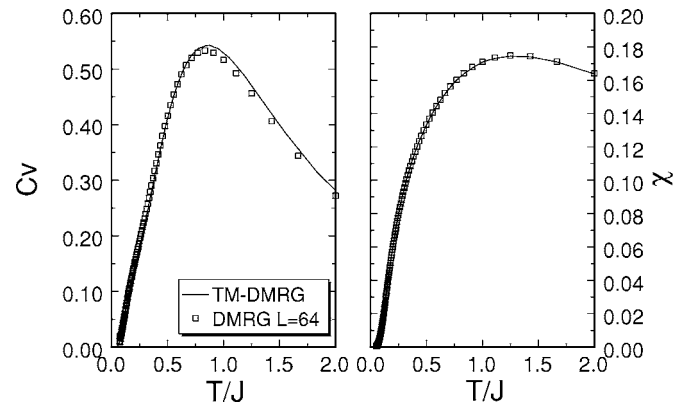


FIG. 1. Specific heat and magnetic susceptibility of the  $S=1$  spin chain of length  $L=64$  obtained with the Suzuki-Trotter time-evolution algorithm. We compare with results from TM-DMRG in the thermodynamic limit.

heat at  $T=0.1$ , which is a measure of the fluctuations in the energy, for different truncation errors. Although the errors in the energy appear small, they are amplified in the calculation of the specific heat. In most of the simulations we have used a time step of  $\tau=0.1$ , but we have also used smaller values to check the effects of the Suzuki-Trotter error, as we discuss below. We have also used variable time steps in the time-targeting method, from  $\tau=0.01$  for high temperatures up to  $\tau=0.2$  for low  $T$ .

To illustrate the method, we begin by looking at the spin  $S=1$  Heisenberg chain, using the Trotter time evolution method. We compare with the TM-DMRG results of Xiang.<sup>16</sup> The TM-DMRG results have a small, well-controlled Trotter error owing to the formation of the transfer matrix; similarly, our time evolution has a different small, well-controlled Trotter error. The TM-DMRG results are in the thermodynamic limit, whereas our results here were on a  $L=64$  site system with open boundary conditions.

We calculated the specific heat  $C_V$  by taking the numerical derivative of the energy with respect to the temperature, using energy differences between adjacent time steps. In order to avoid edge effects we calculated the local energy in the

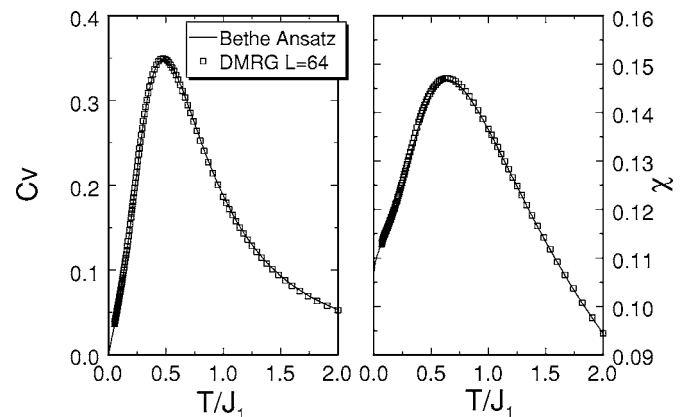


FIG. 2. Specific heat and magnetic susceptibility of a  $S=1/2$  spin chain of length  $L=64$ , compared to exact  $L=\infty$  results using the Bethe ansatz.

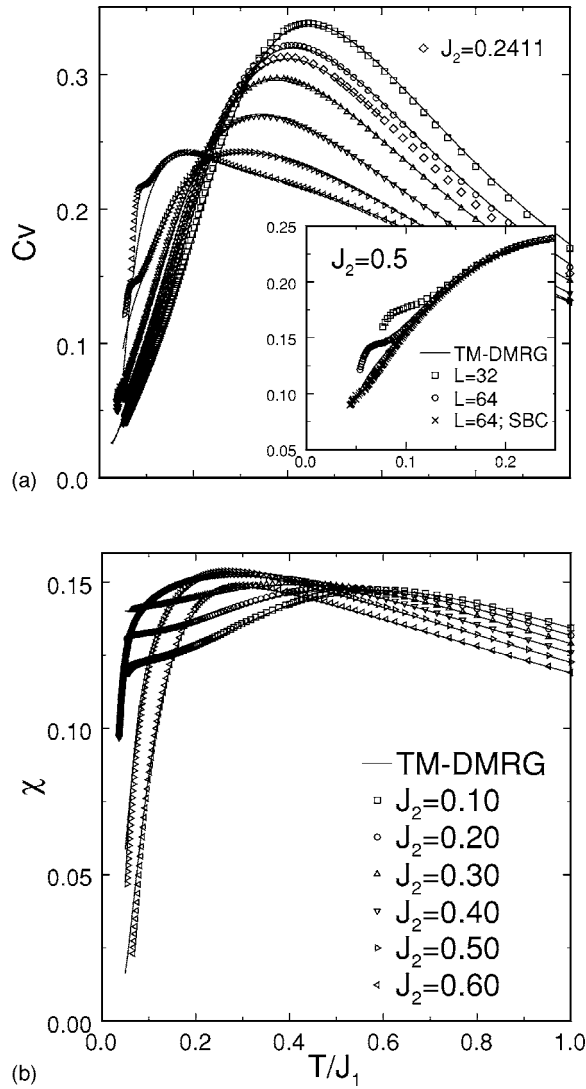


FIG. 3. Specific heat and magnetic susceptibility of a frustrated  $S=1/2$  spin chain of length  $L=64$  obtained using time-step targeting, compared to results from transfer-matrix DMRG (Refs. 3 and 21). Inset: results for  $J=0.5$  for different chain lengths and smooth boundary conditions.

center of the chain. We also calculated the magnetic susceptibility, using the formula

$$\chi(T) = \frac{1}{T} \sum_i \langle S_0^z S_i^z \rangle,$$

where the correlations were calculated at equidistant points from the center of the open chain, following the procedure described in Ref. 17. We have used half integer spins at both ends, as in Ref. 18. Results for these thermodynamic quantities are plotted in Fig. 1. The agreement between our results and Xiang's TM-DMRG is very good for both quantities, for temperatures down to  $T \approx 0.05$ . At high  $T$  we see slight deviations; we have checked our results at high  $T$  using smaller time steps and have found no difference, so we believe the differences are due to Trotter error in the TM-DMRG.

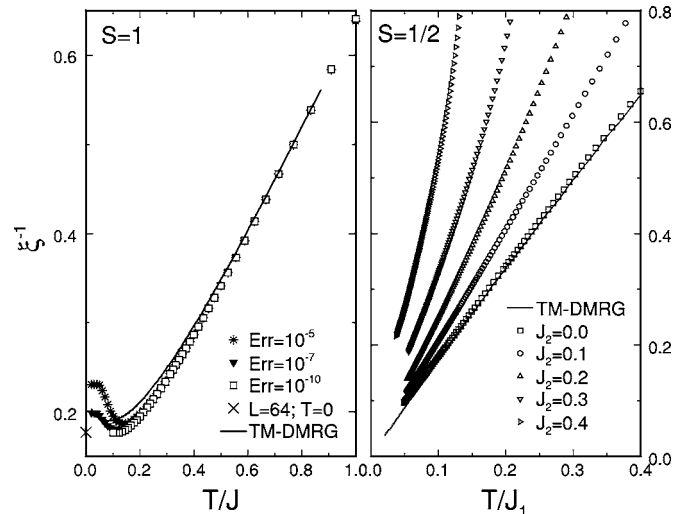


FIG. 4. Correlation length as a function of the temperature for the  $S=1$  Heisenberg chain (left panel), and the frustrated Heisenberg chain (right panel), for different values of  $J_2/J_1$ . Our calculations are on finite chains of length  $L=64$ . We add for comparison results from TM-DMRG in the thermodynamic limit. For  $S=1$  we show results using different truncation errors, and at  $T=0$  from ground state DMRG.

As a second test example, we choose the spin- $\frac{1}{2}$  Heisenberg chain with nearest- and next-nearest-neighbor interactions, with the Hamiltonian

$$H = \sum_i J_1 S_i \cdot S_{i+1} + J_2 S_i \cdot S_{i+2}. \quad (5)$$

Since it is not trivial to use the Suzuki-Trotter break up for the frustrated case, we used the time-step targeted method.<sup>15</sup>

In Fig. 2 we compare our results for  $C_V$  and  $\chi$  for the unfrustrated chain ( $J_2=0$ ) with results from the Bethe ansatz calculations of Ref. 19 in the thermodynamic limit. The agreement is excellent for the entire range of temperatures studied. Finite-size effects were not apparent down to  $T \approx 0.1$ .

When frustration is introduced, it is well known that this model is gapless for  $J_2 \leq J_{2c} \approx 0.2411J_1$ . At this value the chain breaks the translational symmetry by dimerizing, and an exponentially small gap opens.<sup>20</sup> At the point  $J_2=0.5J_1$  the exact ground states become two dimer coverings, and the correlations extend only to one lattice spacing. The frustration present in this model makes reliable quantum Monte Carlo simulations very difficult, due to the appearance of the minus sign problem, and the most accurate results for thermodynamics quantities have been obtained using transfer-matrix DMRG.<sup>3,21</sup>

In Fig. 3 we show our results for the specific heat and susceptibility for different values of frustration  $J_2$ , below and above the critical point  $J_{2c}$ . Notice that due to dimerization, we have to symmetrize two correlations for each distance,  $\langle S_i^z S_j^z \rangle$  and  $\langle S_{i+1}^z S_{j+1}^z \rangle$ . For small values of frustration,  $J_2 \leq J_{2c}$ , the chain behaves as in the unfrustrated case, and

the agreement is excellent, even for values of frustration up to  $J_2=0.5J_1$ . At this point we see more evident finite-size effects reflected in the curves by a hump that appears in the specific heat at small temperatures. A detailed study of this hump shows that this is indeed a finite-size effect, since it moves to lower temperatures as we increase the size of the chain as shown in the inset in Fig. 3. At this value of the frustration, the ground state is degenerate in the thermodynamic limit, or in chain with periodic boundary conditions. This degeneracy is lifted in finite chains with open boundary conditions. Similar characteristics can be observed in Ising chains, where the two Neel configurations are ground states, when a small off-diagonal coupling is introduced.<sup>22</sup> By imposing a version of smooth boundary conditions,<sup>23</sup> where we turn on  $J_2$  slowly and smoothly from 0.0 at the edges to  $0.5J_1$  in the central region, we are able to eliminate the hump.

With our technique detailed spatial correlations functions are as easily obtained as with ground state DMRG. We have calculated the spin-spin correlations and fit them to an expression of the form

$$C(r) \approx A \exp(-r/\xi). \quad (6)$$

Figure 4 shows the results for  $\xi^{-1}$  vs  $T$  for  $S=1$  and  $S=1/2$ . The agreement with the results from TM-DMRG is excellent. For  $S=1$  we notice the same minimum observed in the TM-DMRG simulation by Xiang.<sup>16</sup> We studied the system using time targeting and also reducing the time step, and we found that the source of that minimum can be attributed to the DMRG truncation error, as can be seen in the figure.

To summarize, we have described a DMRG algorithm to study strongly correlated quantum systems at finite temperatures by using an enlarged Hilbert space with ancillary degrees of freedom. We have illustrated its application by calculating thermodynamic quantities of gapless and gapped systems, including frustration. The ideas presented here are simple to implement as an extension to standard DMRG codes, and are not restricted to nearest-neighbor interactions or to single chains.

We thank J. Sirker for useful comments. We acknowledge the support of the NSF under Grant No. DMR03-11843.

<sup>1</sup>S. R. White, Phys. Rev. Lett. **69**, 2863 (1992), Phys. Rev. B **48**, 10345 (1993).

<sup>2</sup>T. Nishino, J. Phys. Soc. Jpn. **64**, L3598 (1995); R. J. Bursill *et al.*, J. Phys.: Condens. Matter **8**, L583 (1996); X. Wang and T. Xiang, Phys. Rev. B **56**, 5061 (1997).

<sup>3</sup>K. Masinger and U. Schollwöck, Phys. Rev. Lett. **81**, 445 (1998).

<sup>4</sup>G. Vidal, Phys. Rev. Lett. **91**, 147902 (2003); **93**, 040502 (2004).

<sup>5</sup>M. Zwoiak and G. Vidal, Phys. Rev. Lett. **93**, 207205 (2004).

<sup>6</sup>F. Verstraete, D. Porras, and J. I. Cirac, Phys. Rev. Lett. **93**, 227205 (2004).

<sup>7</sup>F. Verstraete, J. J. Garcia-Ripoll, and J. I. Cirac, Phys. Rev. Lett. **93**, 207204 (2004).

<sup>8</sup>S. Östlund and S. Rommer, Phys. Rev. Lett. **75**, 3537 (1995).

<sup>9</sup>S. R. White and A. E. Feiguin, Phys. Rev. Lett. **93**, 076401 (2004).

<sup>10</sup>A. J. Daley *et al.*, J. Stat. Mech.: Theory Exp. 2004, P04005.

<sup>11</sup>F. Verstraete *et al.*, cond-mat/0407066 (unpublished).

<sup>12</sup>Y. Takahashi and H. Umezawa, Collect. Phenom. **2**, 55 (1975); H. Umezawa, H. Matsumoto, and M. Tachiki, *Thermo Field*

*Dynamics and Condensed States* (North-Holland, Amsterdam, 1982); H. Matsumoto, in *Progress in Quantum Field Theory* (North-Holland, Amsterdam, 1986), p. 171.

<sup>13</sup>M. Suzuki, J. Phys. Soc. Jpn. **12**, 4483 (1985), and references therein.

<sup>14</sup>S. M. Barnett and P. L. Knight, Phys. Rev. A **38**, 1657 (1988); J. Opt. Soc. Am. B **2**, 467 (1985).

<sup>15</sup>A. E. Feiguin and S. R. White, Phys. Rev. B **72**, 020404(R) (2005).

<sup>16</sup>T. Xiang, Phys. Rev. B **58**, 9142 (1998).

<sup>17</sup>S. R. White and D. A. Huse, Phys. Rev. B **48**, 3844 (1993).

<sup>18</sup>S. R. White, Phys. Rev. B **48**, 10345 (1993).

<sup>19</sup>A. Klümper and D. C. Johnston, Phys. Rev. Lett. **84**, 4701 (2000).

<sup>20</sup>S. R. White and I. Affleck, Phys. Rev. B **54**, 9862 (1996), and references therein.

<sup>21</sup>N. Maeshima and K. Okunishi, Phys. Rev. B **62**, 934 (2000).

<sup>22</sup>J. C. Bonner and M. E. Fisher, Phys. Rev. **135**, A640 (1964).

<sup>23</sup>M. Vekić and S. R. White, Phys. Rev. Lett. **71**, 4283 (1993).